City Car Drag Reduction by means of Flow Control Devices

2020-36-0080

City Car Drag Reduction by means of Flow Control Devices

Alessandro Ferraris, Henrique de Carvalho Pinheiro, Andrea Giancarlo Airale and Massimiliana Carello
Politecnico di Torino - Mechanical and Aerospace Engineering Department

Davide Berti Polato
Beond Srl. - Italy

Abstract

In the past few decades, the automotive industry saw the development of several environment-friendly technologies, as high efficiency engines, lightweight materials, and low-rolling-resistance tires. Car body styling, together with aerodynamics, play an important role in resolving environmental issues by reducing drag force, which results in high fuel efficiency and lower energy requirements. The main objective of this study is the reduction of the aerodynamic resistance of a city-car prototype by means of flow control devices (air blow and air relief) located into the wheel arches. This work starts from the wind tunnel experimental tests of the baseline version of the XAM 2.0 vehicle, then, dedicated ducts are implemented into the model in order to reduce the turbulence of the front wheel well and the air-flow defection at the end of the sides of the car body. A CFD analysis is carried out in order to assess the effects of the introduced modifications: car shape is varied by CAS, for every modification CFD calculations are performed. A correlation between wind tunnel and CFD results is carried out validating the drag optimization, demonstrating the predictive capabilities of CFD analysis and a record-breaking drag coefficient.

Introduction

Currently the issue of mobility is one of the most delicate and controversial topics in the worldwide debate. Great steps have been taken to improve vehicle efficiency, on drag reduction [1], use of lightweight materials for innovative and conventional components [2] [3], as well as different powertrain architectures and control strategies [4,5].

This paper focuses on the reduction of energy consumption through aerodynamic drag lowering, which will then correspond to a mileage increment. As an example, a reduction of 0,01 of the C_D [6] corresponds to an 0,85 kilometer per liter improvement of fuel economy [7].

The vehicle under study is XAM 2.0. It has been designed for an open road use, integrating know-how and the most successful aerodynamic features from the previous version (XAM), developed by the H_2politO team to race in the urban concept category of the Shell Eco-marathon competition [8,9].

XAM 2.0 is an Extended-Range Electric Vehicle (E-REV) with a brushless Interior Permanent Magnet (IPM) and a Wankel thermal engine, homologated as heavy quadricycle SUB-A segment (L7e) [10]. Overall external size (LxWxH) is 2, 880x1, 300x1, 280 meters with a total mass of 600 kg. It is worth noting its particularly low

aspect ratio, due to the reduce wheelbase of this urban concept, that renders especially difficult the drag reduction and aerodynamic correlation.

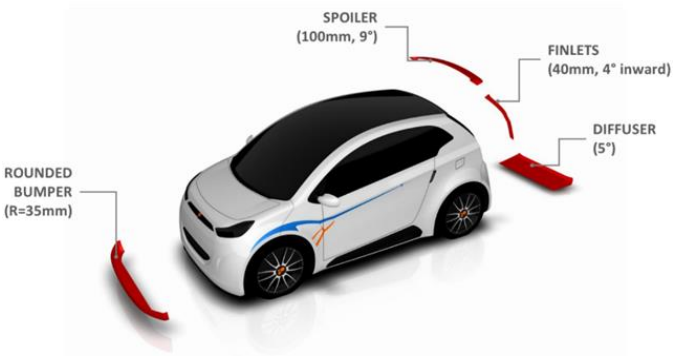

Figure 1 - Baseline aerodynamic features of XAM 2.0

A previous study has performed an analysis in the same vehicle, adding to the understanding regarding its aerodynamic characteristics [11]. There, four aerodynamic add-on devices were evaluated to reduce the vehicle's drag and their performance optimized: spoiler, finlets, front bumper and rear diffuser (Figure 1).

One of its key conclusion is that, although there are some inherent differences between the CFD and Wind Tunnel tests overall C_D values (ranging between 20 and 25% error), the method allows a very precise conclusion about the net impact of new features in drag reduction (always below 1% discrepancies).

The present study has been developed using the same approach: a CFD simulation and real wind tunnel tests of the vehicle prototype, which permits a numerical-experimental validation of results and a further reduction of the drag resistance. To achieve this goal, two zones were analyzed (front wheel wells and rear bumper curvature), some issues in their flow were identified and flow control devices (aero-curtains [12], air relief / breather [13], and rear air blow) were proposed to enhance their aerodynamic performance.

Methodology Description

The analysis has been performed with a two-prong approach:

- CFD simulations were performed with STAR-CCM+ software;
- Experimental tests were conducted in the Pininfarina wind tunnel located in Grugliasco (Turin).

The domain for CFD simulations includes the virtual wind tunnel and the car model. Thanks to model symmetry, the simulated domain was halved, leading to a significant reduction of computational effort. As suggested in [14] and [15], domain dimensions LxWxH are 33,5x6x6 meters, considering the car size previously reported.

The surface mesh of the physics continuum was generated using ANSA-BetaCae software, while the volume mesh was created in the pre-processor of STAR-CCM+, using several refinement boxes in order to create a

ISSN 0148-7191

finer mesh in regions that required higher accuracy (Figure 2), with sizes from 8 to 50 mm and a base size of 1 meter.

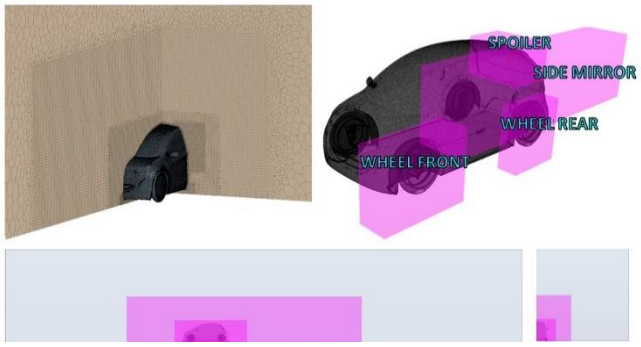

Figure 2 - Mesh volume refinements

In order to obtain the expected wall y+ range suggested by [16] and [17], 3 prism layers around the car were created: the thickness of near wall layer was 3 mm and total was 20 mm.

The obtained wall y+ range is shown in Figure 3, respectful of the Star-CCM+ guidelines. The final volume mesh model has 8 millions of polyhedral elements.

To better correlate the fluid domain of the simulation with real wind tunnel tests, the following boundary conditions were chosen:

- Moving floor;
- Moving Wheels;
- Uniform velocity (50 km/h) at the inlet;
- Temperature of air: 250C;
- Density of air: 1.184 kg/m^3;
- Viscosity of air: 1.855e-5 Pa-s;
- Ambient static pressure at the outlet;
- Turbulence model: Reynolds-Averaged Navier-Stokes (RANS) with Realizable K-Epsilon [15].

ISSN 0148-7191

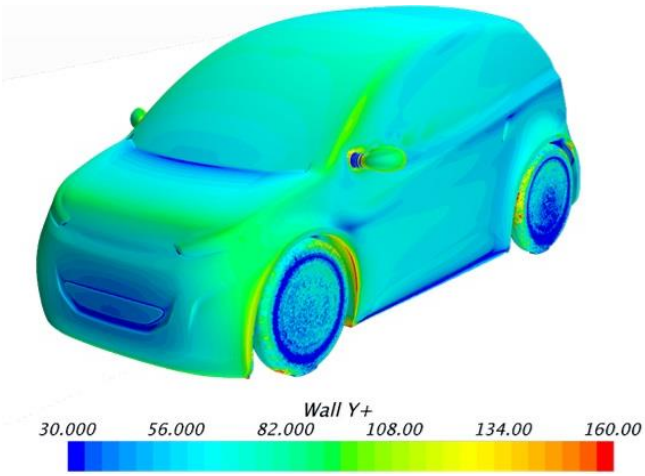

Figure 3 - Wall y+ range values

In order to monitor the convergence of the solution, two reports with relative plots have been created, one for drag force (D) of the entire vehicle and the other for its coefficient (C_D).

The processing was run for 3000 iterations with final residuals lower than $1e^{-4}$, resulting in D = 20,68 N and C_D = 0,253 for the baseline vehicle.

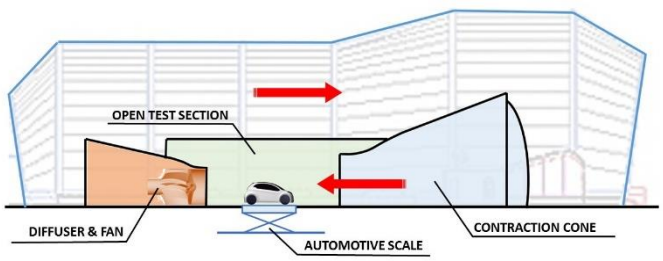

Figure 4 - Pininfarina wind tunnel scheme

The experimental WT tests are schematically depicted in Figure 4. Its floor presents a moving belt called T-belt [18, 19] due to the shape that is formed by a central belt and two lateral belts in the front of the car. These reproduce the ground effect condition seen in real world conditions.

The wheels are positioned on rollers that are connected to a three-axes dynamometer. This provides the three components of the force induced on the vehicle by aerodynamic effects (lift, drag and skin friction) and exchanged with the ground through the wheels. In this way, it is possible to evaluate for each test with precision:

- The overall drag force (D) acting on the vehicle and the corresponding coefficient (C_D);
- The lift forces acting on front (LF) or on rear (LR) axles;
- The overall lift force (L) acting on the vehicle and the corresponding coefficient (C_L).

ISSN 0148-7191

The tests were carried out at three different speeds (30, 50 and 70 km/h), using a 14-holes probe at a distance of 150 mm behind the vehicle for data acquisition, as shown in Figure 5.

Figure 5 - Pressure field measurement with 14-holes probe

A first round of tests and simulations is performed and the overall comparison between CFD and wind tunnel results gave good correlation in terms of drag coefficient, validating the followed methodology. This is confirmed by the results shown in Table 1.

Table 1 - CFD-WT correlation of C_D

Speed	CFD	WT	Δ(CFD-WT)
30 km/h	0,260	0,328	20,7%
50 km/h	0,263	0,325	19,1%
70 km/h	0,264	0,325	18,8%

One of the reasons that could explain the variation is the already cited low aspect ratio of the vehicle, due to its short wheelbase, in addition to a vehicle designed to an urban environment and having its typical velocities lower than the average passenger car (and consequently also the Reynolds Number).

As expected, due to these considerations, the gap between virtual and experimental values decreases as speed increases. However, the authors were not able to explore the error reduction trend and increase the test velocity, due to the risk of losing representativeness to the real application. In any case, the absolute value remains below the previous reference for this vehicle [11]. All the CFD simulations and WT tests henceforth presented were obtained at 50km/h.

Once the methodology is described and validated it is possible to use their results to better understand the flow in the two main areas of interest and come up with possible solutions, as described in the next two sections.

ISSN 0148-7191

Rear Bumper Flow

Concerning the rear part of the vehicle, both WT and CFD (Figure 6) results showed a high vorticity and flow deflection at the rear of the car, which seems to be responsible for vortexes creation in the wake.

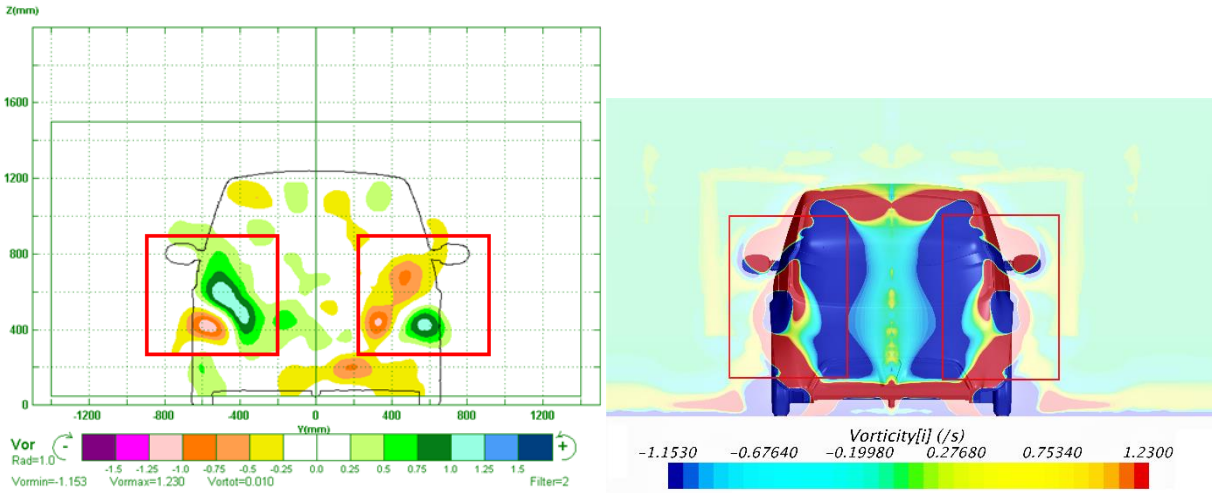

Figure 6 - Correlation between WT (up) and CFD (down) vorticity 150 mm behind the vehicle

Indeed, the flow exiting from the car sides behind the belt line was highly deflected, due to the rounded shape of the bumper, as observable in Figure 7 where it is possible that the airflow has a lateral component that forces it to curve inward.

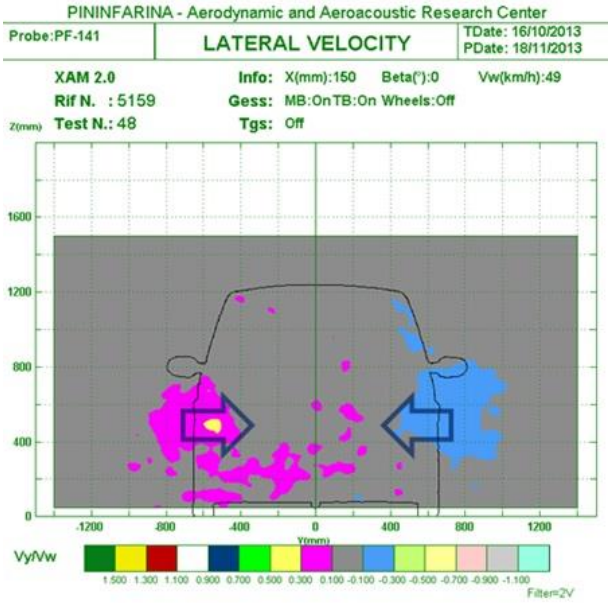

Figure 7 - Airflow lateral velocity measured in WT

ISSN 0148-7191

Further analysis, not reproduced in this paper for sake of brevity, has been performed and a horizontal cross section under the car belt line confirms the high turbulent kinetic energy produced in this area. Finally, the micro-drag distribution confirmed a significant dissipation in both car sides.

These tests put together suggest that the model has an additional potential for lowering drag. To be able to achieve this goal, a mean to detach the airflow, thus avoiding deflection, is needed: it can be obtained either with a physical edge or a properly oriented flow. The latter is preferred, and an air blower is conceptualized. The objective of this device is to take advantage of the high-pressure turbulent flow naturally present in the rear wheel well by directing it towards the critical zone by means of an internal duct.

The presence of this new air source tends to energize the lateral flow and detach it before the curved section of the bumper, avoiding the formation of a lateral component of its velocity. This extraction from the wheel wells can also be beneficial to the flow around the wheel itself. The final air blower is presented in Figure 8.

Figure 8 - Rendering of the concept at the basis of the rear air blow

ISSN 0148-7191

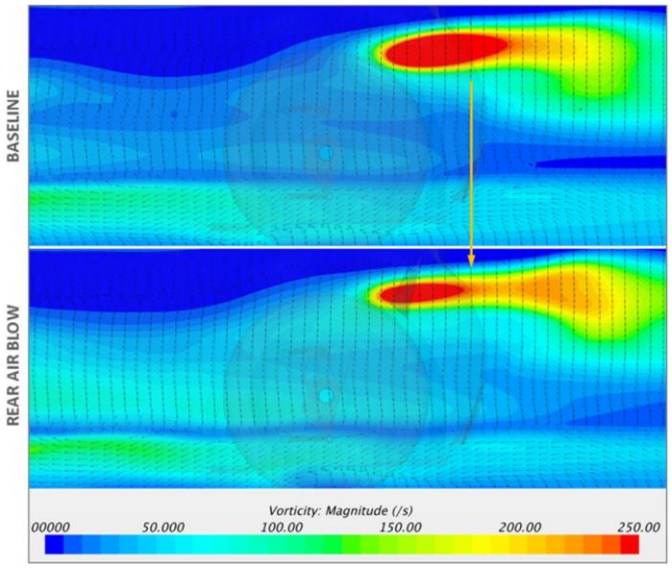

Figure 9 - Vorticity distribution in correspondence of the rear wheel well

The CFD analysis provides a numeric confirmation of the desired effect: the vorticity caused by flow deflection around the bumper surface is reduced if the rear air blow is present, yielding a resistance reduction. Figure 9 shows the reduction in the vorticity after the implementation of the device.

Front Wheel Wells Flow

The flow near the wheel arches also presents turbulence, due to the air that exits from the wheel wells. This uncontrolled flow interacts with the side flow and introduces other disturbances along the car sides. The evidence of this effect is shown in wind tunnel thanks to the smoke visualization (Figure 10 up), confirming the CFD simulation results (Figure 10 down).

ISSN 0148-7191

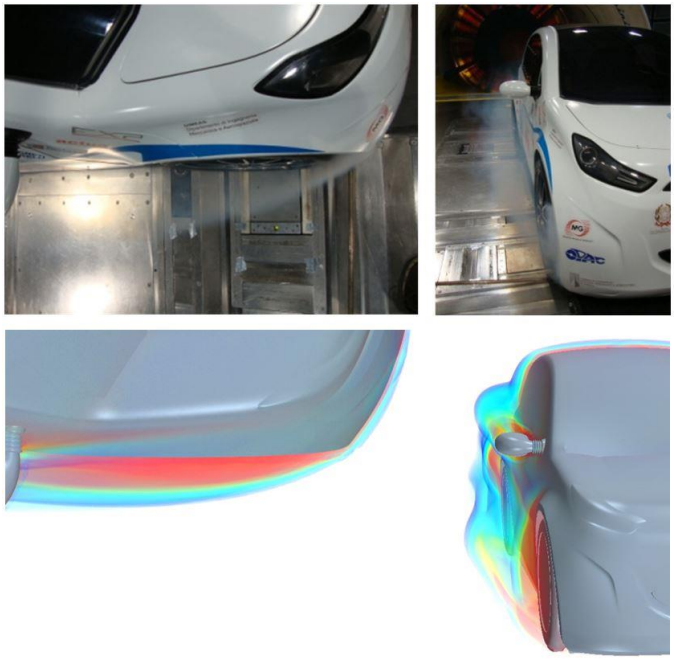

Figure 10 - Correlation between smoke visualization in WT (up) and vorticity rendering in CFD (down) in correspondence of the front wheel-case in top view and front view

An aerodynamic device able to dissipate the turbulence can be introduced upstream the wheel, into the front bumper, similarly to the solution used in the rear part.

The aero curtain and air relief are aerodynamic devices aimed at front wheel well flow control; they should reduce the turbulence created by the rotation of the wheel in the side flow and wake. In Figure 11 the concept at the basis of the air curtain design is illustrated.

The front air curtain consists in a channel with inlet in the car front, where high pressure is present. The convergent geometry of the duct accelerates the air flow, which exits at the edge of the wheel case oriented along the external face of the tire. This creates the air curtain that reduce the turbulence of the wheel.

The air relief instead will behave similarly to the air blower previously presented, but in this case mainly focused on avoiding a high-pressure zone disturbance in the wheel arches, by extracting the air towards the side of the vehicle in a controlled direction.

ISSN 0148-7191

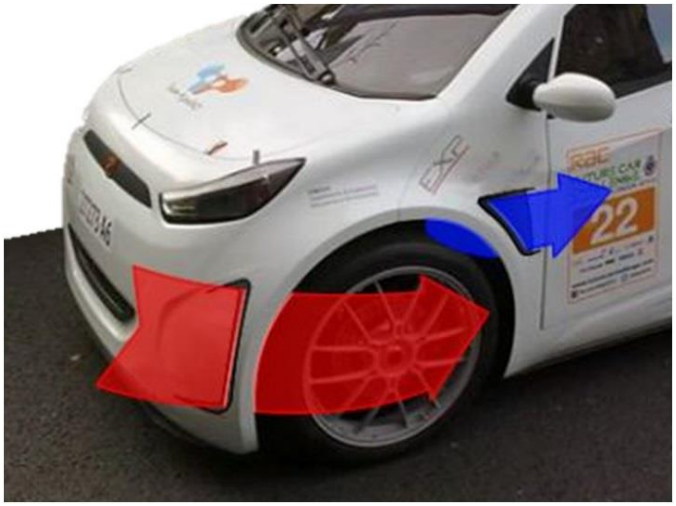

Figure 11 - Design concept of the air curtain (red) and air relief (blue)

The resulting side flow is expected to be less prone to detach, resulting in a lower dissipation and drag coefficient. The CFD analysis of XAM 2.0 vehicle prototype confirmed the effects of the devices implemented, as is possible to notice comparing the original air velocities in the front wheel zone with the baseline model in Figure 12 (top) and after the application of the air blow as showed in Figure 12 (bottom). Particularly the red-circled area demonstrates that the air curtain can dissipate the turbulence and guarantees a more streamlined flow along car sides.

The results in terms of drag reduction of the design phase are reported in Table 2.

Table 2 – C_D values of the different simulated models (CFD)

Model	C_D	ΔC_D
Baseline	0,2586	-
Front Air Curtain and	0,2571	0,0015
Front and Rear Air	0,2561	0,0010
Final Model	0,2561	0,0025

This result is further supported by the turbulent kinetic energy volume rendering in Figure 13, which shows that the wheel well disturbances are significantly reduced when the air curtain and air relief are present (right).

ISSN 0148-7191

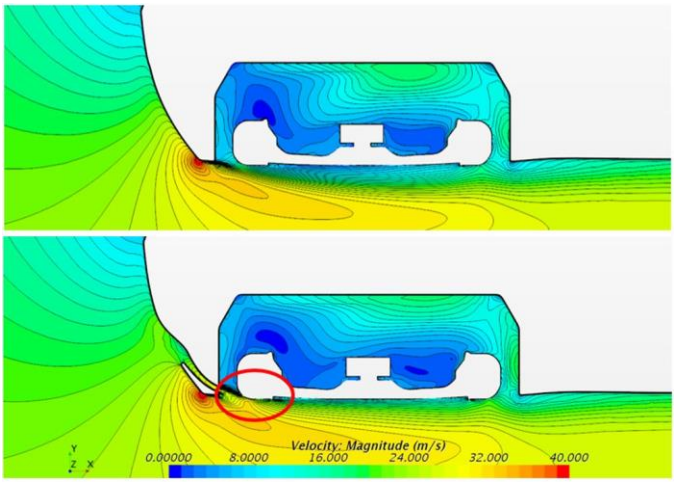

Figure 12 - Velocity magnitude and streamlines in correspondence of the front wheel-case in the baseline model (top) and with air curtain and air relief (bottom)

The total aero-drag reduction obtained with CFD simulations is about 1% of the baseline drag coefficient; the aerodynamic resistance will be reduced accordingly.

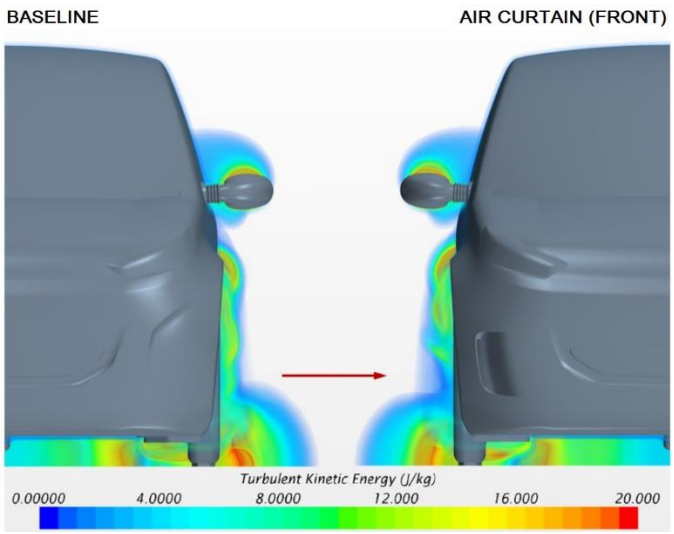

Figure 13 - Turbulent kinetic energy volume rendering

Conclusion

The study presented in this paper confirmed that innovative aerodynamic features for flow-control integrated into car model allow to reduce drag. Their implementation often requires a small increase in production cost, since they consist of light modification of the existing car body components.

ISSN 0148-7191

Aero curtain and air relief are aerodynamic solutions that became an innovative style feature for the new generation of cars. The front air blow has been integrated in the car front so to obtain a functional and visually appealing technical solution. Front and rear air blows were integrated in XAM 2.0 by modifying the car body and inserting the ducts produced with rapid prototyping techniques.

Concerning the methodology, the physical evidence of the disturbances around the model were demonstrated first by the experimental tests in a wind tunnel, and then confirmed by the CFD simulations, also in terms of effects of the flow control devices.

The combined use of experimental tests and virtual simulation is very powerful from the methodology point of view. In particular, CFD simulations are a very useful tool, since they can provide fast and accurate prediction of the aerodynamic performance of the car (even during the design phase, when the physical model is not yet available), particularly when the relation between physical and virtual (CFD) results is known, permitting an efficient cost-time approach.

Future aerodynamic development of the XAM 2.0 project will be a final validation of the optimized studied flow control devices in new set of WT tests.

References

1. Schuetz, T., “Aerodynamics of road vehicles”, Published by SAE International, fifth edition. Warrendale, Pennsylvania, pp. 1312, 2016, ISBN:978-0-7680-7977-7.
2. Carello, M., Airale, A., and Ferraris, A., "City Vehicle XAM 2.0: Design and Optimization of the Composite Suspension System," SAE Technical Paper 2014-01-1050, 2014, doi:10.4271/2014-01-1050.
3. Carello, M., Airale, A.G., Ferraris, A. et al. “Static Design and Finite Element Analysis of Innovative CFRP Transverse Leaf”, Spring. Appl Compos Mater 24, 1493–1508, 2017, doi:10.1007/s10443-017-9596-6
4. Carello, M., Ferraris, A., Airale, A., and Fuentes, F., "City Vehicle XAM 2.0: Design and Optimization of its Plug-In E-REV Powertrain," SAE Technical Paper 2014-01-1822, 2014, doi:10.4271/2014-01-1822.
5. Carello, M., Airale, A.G., Ferraris, A., and Messana, A., “XAM 2.0: from Student Competition to Professional Challenge,” Computer-Aided Design and Applications, vol. 11, pp. S61–S67, 2014, doi:10.1080/16864360.2014.914412
6. Road Vehicle Aerodynamics Forum Committee, “Vehicle Aerodynamics Terminology,” SAE Standard J1594, Rev. Oct. 2010, doi:10.4271/J1594_201007
7. S. Elliot-Sink, “Improving Aerodynamics to Boost Fuel Economy,” Edmunds, 2011, available at: http://www.edmunds.com/fuel-economy/improving-aerodynamics-to-boost-fuel-economy.html?articleid=106954&.
8. Carello, M., Andrea, S., Airale, A., and Ferraris, A., "Design the City Vehicle XAM using CFD Analysis," SAE Technical Paper 2015-01-1533, 2015, doi:10.4271/2015-01-1533.
9. Carello, M., “Innovative and Multidisciplinary Teaching Through the Design and Construction of Low Consumption Vehicles for International Competitions”, New Trends in Educational Activity in the Field of Mechanism and Machine Theory, pp 72-79, 2018, doi:10.1007/978-3-030-00108-7.
10. European Parliament, “on the approval and market surveillance of two- or three-wheel vehicles and quadricycles”, Official Journal of the European Union, L 60/52, Regulation (EU) No 168/2013, 2013, ELI: http://data.europa.eu/eli/reg/2013/168/oj
11. Ferraris, A., Airale, A. G., Berti Polato, D., Messana, A., et al. “City Car Drag Reduction by Means of Shape Optimization and Add-On Devices”. Uhl T. (eds) Advances in Mechanism and Machine Science. IFToMM

ISSN 0148-7191

WC 2019. Mechanisms and Machine Science, vol 73. Springer, Cham, 2019, doi:10.1007/978-3-030-20131-9_367
12. Morey, B., “Advanced aerodynamics features applied to Mustang,” SAE International, March 2014. Available at: https://www.sae.org/news/2014/03/advanced-aerodynamics-features-applied-to-mustang
13. Schütz, T., Klußmann, S. and Neuendorf, R, “Automotive Aerodynamics in 2020”, ATZ Worldw 118, 48–53 (2016). doi:10.1007/s38311-016-0144-z.
14. Blocken, B. and Toparlar Y.,”A following car influences cyclist drag : CFD simulations and wind tunnel measurements” J. Wind Eng. Ind. Aerodyn., 145 (2015), pp. 178-186, 2015, doi:10.1016/j.jweia.2015.06.015
15. Siemens Software PLM, “Incompressible external aerodynamics: Steady state RANS approach”, STAR-CCM+ guidelines for aerodynamics calculations, User Guide 11_06, 2016.
16. Ahmad, N.E., Abo-Serie, E. and Gaylard, A., “Mesh optimization for ground vehicle Aerodynamics”, CFD Letters, vol 2, no. 1, pp. 54-65, 2010, ISSN:2180-1363
17. Connor, C., Kharazi, A., Walter, J., and Martindale, B., "Comparison of Wind Tunnel Configurations for Testing Closed-Wheel Race Cars: A CFD Study," SAE Technical Paper 2006-01-3620, 2006, doi:10.4271/2006-01-3620.
18. Cogotti, A., "Ground Effect Simulation for Full-Scale Cars in the Pininfarina Wind Tunnel," SAE Technical Paper 950996, 1995, doi:10.4271/950996.
19. Cogotti, A., "The New Moving Ground System of the Pininfarina Wind Tunnel," SAE Technical Paper 2007-01-1044, 2007, doi:10.4271/2007-01-1044.

Contact Information

Politecnico di Torino – Department of Mechanical and Aerospace Engineering
C.so Duca degli Abruzzi, 24 -10129 Torino – Italy
Phone: +39.011.0906946

Massimiliana Carello
massimiliana.carello@polito.it

Alessandro Ferraris
alessandro.ferraris@polito.it

Henrique de Carvalho Pinheiro
henrique.decarvalho@polito.it

Andrea Giancarlo Airale
andrea.airale@polito.it

Beond Srl.
C.so Castelfidardo 30/a – 10129 – Torino – Italy
Phone: +39 011 198 26 593

Davide Berti Polato
davide.bertipolato@beond.net

ISSN 0148-7191

Acknowledgments

Special thanks to Beta-CAE, Star-CCM+ and Pininfarina for their support.

ISSN 0148-7191

Definitions/Abbreviations

CAD	Computer Aided Design
CAE	Computer Aided Engineering
CAS	Computer Aided Styling
C_D	Coefficient of Drag
C_L	Coefficient of Lift
CFD	Computational Fluid Dynamics
DOE	Design of Experiment
E-REV	Electronic – Range extended vehicle
GESS	Ground Effect Simulation System
RSM	Response Surface Model
RANS	Reynolds Averaged Navier Stokes
WT	Wind tunnel
XAM	eXtreme Automotive Mobility

ISSN 0148-7191